

# Nanostructuring of Silicon Surface with Femtosecond-Laser-Induced Near-field

Godai MIYAJI, Kaifeng ZHANG, Junya FUJITA, and Kenzo MIYAZAKI

*Advanced Laser Science Research Section, Institute of Advanced Energy, Kyoto University,  
Gokasho, Uji, Kyoto 611-0011, Japan  
E-mail: g-miyaji@iae.kyoto-u.ac.jp*

In the femtosecond laser ablation experiment for silicon in water, we observed formation of two kinds of nanostructure with a fine period of  $\sim 150$  nm and a coarse one of  $\sim 400$  nm. It is found that the fine structure can be formed in a restricted range of low fluence of  $60 - 70$  mJ/cm<sup>2</sup>, and its formation is preceded with the surface corrugation due to the coarse structure. In addition, the period sizes in fine and coarse nanostructures were insensitive to the superimposed shot number of laser pulses, while those are very sensitive to the fluence. The formation process of fine nanostructure is illustrated and analyzed with our model of the periodically enhanced near-field through the excitation of surface plasmon polaritons. The calculated near-field period is in good agreement with that observed in the experiment.

DOI:10.2961/jlmn.2012.02.0012

**Keywords:** femtosecond laser ablation, nanostructuring, near-field, surface plasmon polariton, silicon

## 1. Introduction

In a recent decade, ultrashort-pulse lasers have been used extensively to produce periodic nanostructures on the surface of solids such as dielectrics [1-4], semiconductors [5-10] and metals [11,12], and also inside transparent materials [13,14], where the observed size of nanostructures is much less than the laser wavelength  $\lambda$ , suggesting potential applications of ultrashort-pulse lasers to nano-processing. In particular, the laser nano-processing of silicon (Si) is attractive for a variety of applications, while nanostructuring has been observed for various kinds of materials. Nanostructure formation on Si has been observed in water and oil with superimposed fs laser pulses at low fluence around or less than the single-pulse ablation threshold [6-9]. Several mechanisms of nanostructuring on Si surface have been proposed, but detail of the physical process is not understood well.

Based on a series of experimental studies for hard thin films such as diamond-like carbon and TiN [2,3,15-19], we have shown that near-field enhanced with fs laser pulses plays an essential role to initiate the nanoscale ablation on the target surface [15-17], and the nanoscale periodicity can be attributed to the excitation of surface plasmon polaritons (SPPs) in the surface layer [18].

In this paper, we report an experimental study of nanostructure formation on Si surface in water that has been made to see the nanostructuring process and applicability of our model of nanostructuring to semiconductor materials.

## 2. Experimental

The target used in the experiment was the *p*-type crystalline Si substrate of  $300 \mu\text{m}$  in thickness, which was placed in a small cell filled with distilled water. The Si surface was irradiated through the 2-mm thick water layer

and a quartz window of the cell. We used 800 nm, 100 fs laser pulses with linear polarization from a Ti:sapphire laser system operated at the repetition rate of 10 Hz. The laser pulse was focused on the target surface with a 1000-mm focal-length spherical lens at normal incidence. The focal spot size on the target was  $200 \mu\text{m}$  in radius at  $e^{-2}$  of the maximum intensity with the lowest-order Gaussian intensity profile observed with a CCD camera.

Throughout of the experiment, we used lineally polarized pulses, and the fluence  $F$  on the Si target was less than the single-pulse ablation threshold. Then the ablation of Si surface was induced with superimposed multiple laser pulses. The superimposed shot number  $N$  was in a range of  $N = 1 - 2000$ . The pulse energy was precisely controlled to be in a range of  $16 - 32 \mu\text{J}$  with a pair of the polarizer and a half-wave plate.

We observed in detail the morphological change on Si surface as a function of  $N$  for different fixed values of  $F$  at intervals of  $\sim 5$  mJ/cm<sup>2</sup> or less in a range  $F = 50 - 100$  mJ/cm<sup>2</sup>. The ablated surface was observed with a scanning electron microscope (SEM). To measure the spatial distribution of the structural period  $d$  on the ablated surface, the surface structure of the central  $6 \times 6 \mu\text{m}^2$  area on the focal spot of each SEM image was analyzed with the two-dimensional Fourier transform.

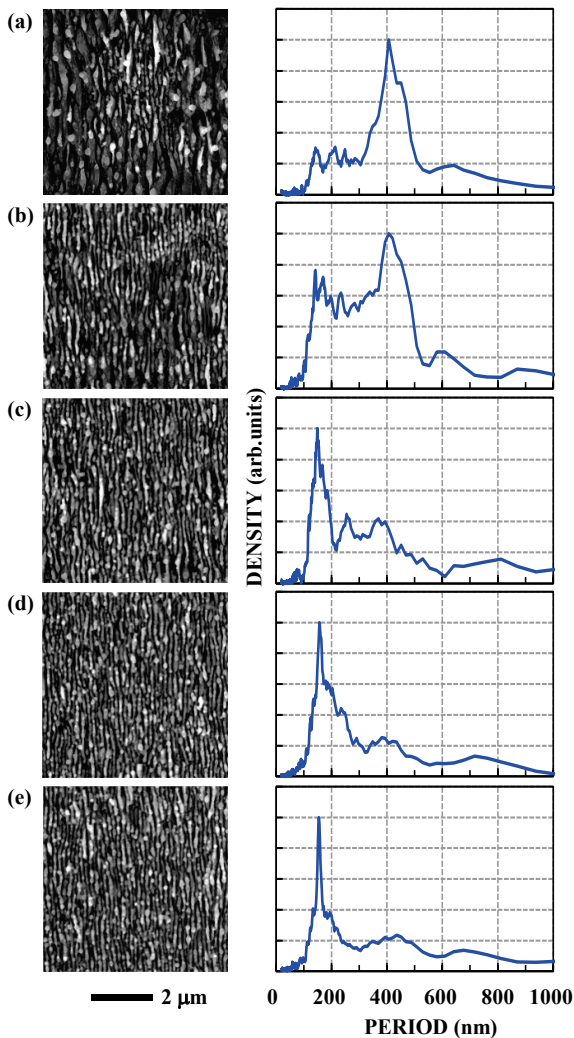
## 3. Results and discussion

Figure 1 shows the SEM image of the ablated Si surface and its power spectrum observed as a function of  $N$  at a fixed fluence of  $F = 60$  mJ/cm<sup>2</sup>, where the spectral peak is normalized by the maximum value.

At the low fluence in Fig. 1, the periodic structures are formed in the direction parallel to the laser polarization. This structure is observed to start to be formed in the central part of the focal spot with  $N = 400$ , where the distribu-

tion of  $d$  represents a broad spectrum in a region of  $d = 130 - 600$  nm with a peak at  $d \sim 400$  nm. With increasing  $N$ , the high-frequency components around  $d \sim 150$  nm increases rapidly to form a structure including double peaks, as seen in Fig. 1(b). With a further increase in  $N$  to 800, the coarse structure density at  $d \sim 400$  nm decreases rapidly in the spectrum, and the surface gets to include a high density of the fine line-like structure with a period of  $d \sim 150$  nm, as shown with the sharp isolated peak in Fig. 1(c). This observation strongly suggests that the coarse structure should be the source of the fine structure. In other words, the fine structure would efficiently be produced with the near-field enhanced around the initially produced coarse structure. This has been confirmed with the results shown in Figs. 1(c) and (d) for  $N = 1000$  and 2000, where the high-frequency peak becomes much sharper, and the whole imaged surface tends to be covered with the fine periodic structure with  $d \sim 150$  nm. It is noted that the fine period  $d$  is almost constant with an increase in  $N$ .

We found that the high-density formation of the fine



**Fig. 1** SEM image of the ablated Si surface (left) and its power spectrum along the laser polarization direction (right) for (a)  $N = 400$ , (b)  $N = 500$ , (c)  $N = 800$ , (d)  $N = 1000$ , and (e)  $N = 2000$  at  $F = 60$  mJ/cm<sup>2</sup>. The image area is  $6 \times 6$  μm<sup>2</sup> on the central focal spot, where the laser polarization direction is horizontal.

nanostructure was observed in a small range of  $F = 60 - 70$  mJ/cm<sup>2</sup>. This indicates that the experimental condition for nanostructuring with  $d \sim 150$  nm is very sensitive to  $F$ . Figure 2 shows the SEM image of Si surface ablated at a higher fixed value of  $F = 75$  mJ/cm<sup>2</sup> and its power spectrum, observed as a function of  $N$ . For  $N = 200$ , the coarse structure is formed in the central focal spot area. The frequency spectrum represents a broad distribution in a range of  $d = 170 - 900$  nm with a peak at  $d \sim 400$  nm, as seen in Fig. 2(a). With increasing  $N$ , the observed spectra appear to maintain the distribution with the density peak at  $d \sim 400$  nm and never include any distinct peak suggesting the fine structure formation. Instead, the spectrum tends to reduce the relative density of higher and lower frequency components to have a sharper peak at  $d \sim 400$  nm, as seen in Fig. 2(b) - (e). It is also noted that the peak position at  $d \sim 400$  nm is almost constant with an increase in  $N$ .

As mentioned above, Si surface in water could be nano-structured under the restricted conditions of  $F$  and  $N$ , especially in a small range of  $F$ . To see in detail the effect

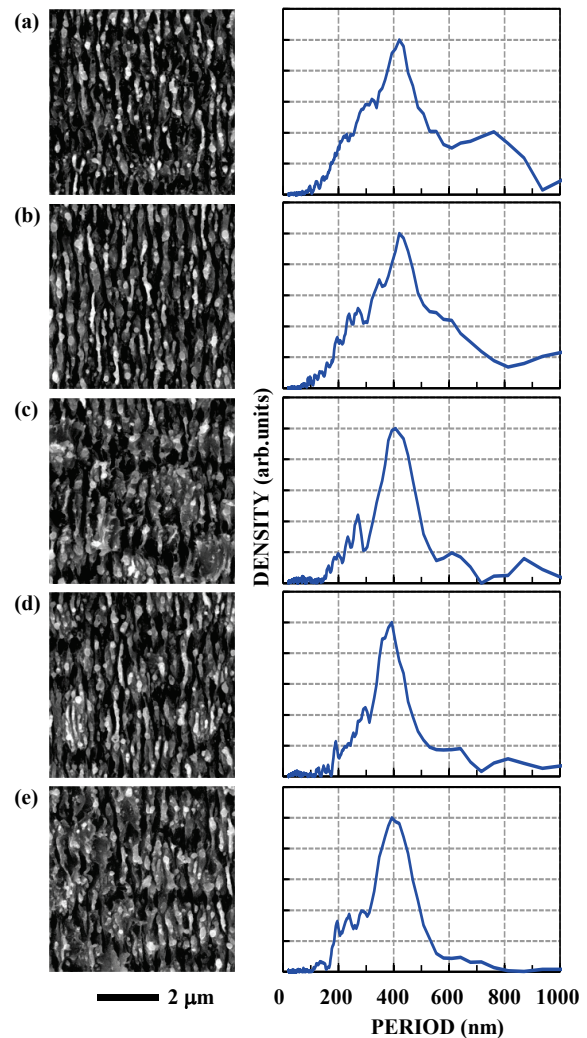


**Fig. 2** SEM image of the ablated Si surface (left) and its power spectrum along the laser polarization direction (right) for (a)  $N = 200$ , (b)  $N = 500$ , (c)  $N = 800$ , (d)  $N = 1000$ , and (e)  $N = 1500$  at  $F = 75$  mJ/cm<sup>2</sup>. The image area is  $6 \times 6$  μm<sup>2</sup> on the central focal spot, where the laser polarization direction is horizontal.

of  $F$  on nanostructuring, the results obtained are compared as a function of  $F$  for a fixed  $N$ . Figure 3 shows an example of the SEM image and its power spectrum that are lined up as a function of  $F$  for  $N = 1000$ . When  $F$  was less than  $60 \text{ mJ/cm}^2$ , Si surface was never ablated with  $N < \sim 2000$ . The ablation to form the nanostructure with  $d \sim 150 \text{ nm}$  started to be observed at  $F \sim 60 \text{ mJ/cm}^2$ , as shown in Fig. 3(a). With a small increase in  $F$ , the density of low frequency components around  $d \sim 400 \text{ nm}$  increases on the surface, as clearly seen in the spectrum shown in Fig. 3(b). At  $F = 70 \text{ mJ/cm}^2$ , however, the high-frequency components in a range of  $d = 150 - 200 \text{ nm}$  still survive in the surface structure, as shown in Fig. 3(c). With increasing  $F$  up to  $75 \text{ mJ/cm}^2$  and higher, the high-frequency components of  $d < \sim 200 \text{ nm}$  decreases, and then the coarse periodic structure with  $d \sim 400 \text{ nm}$  covers the whole imaged area, as seen in Figs. 3 (d) and (e). In addition, the SEM images show a structure with a large period of  $d = 2 - 3 \mu\text{m}$  along the direction perpendicular to the laser polarization

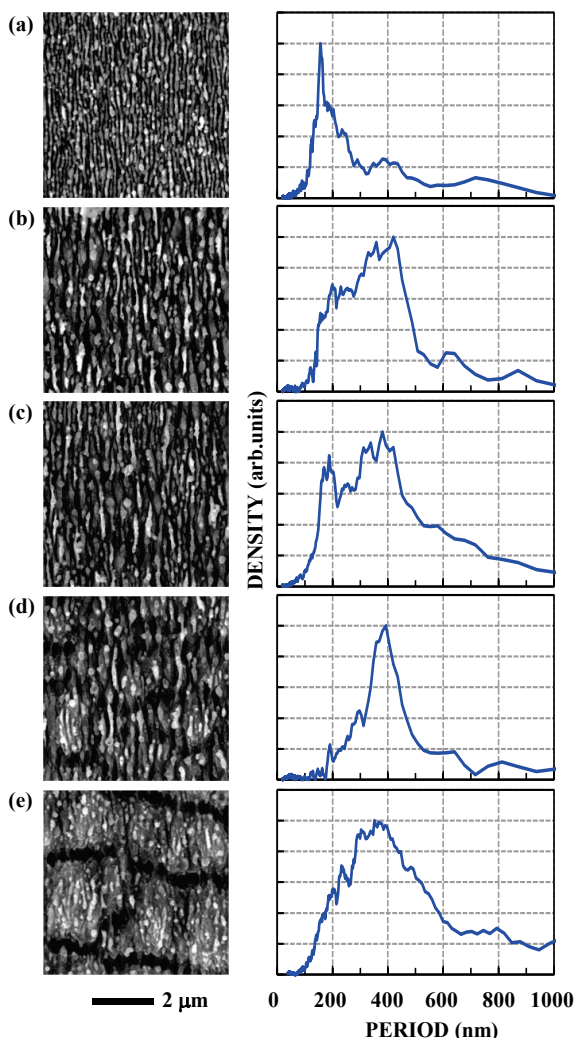


**Fig. 3** SEM image of the ablated Si surface (left) and its power spectrum along the laser polarization direction (right) for  $N = 1000$  at (a)  $F = 60 \text{ mJ/cm}^2$ , (b)  $F = 65 \text{ mJ/cm}^2$ , (c)  $F = 70 \text{ mJ/cm}^2$ , (d)  $F = 75 \text{ mJ/cm}^2$ , and (e)  $F = 80 \text{ mJ/cm}^2$ . The image area is  $6 \times 6 \mu\text{m}^2$  on the central focal spot, where the laser polarization direction is horizontal.

tion.

Thus we conclude that the fine nanostructure formation was possible for Si surface in water by using superimposed multiple fs pulses at a moderate fluence of  $F = 60 - 70 \text{ mJ/cm}^2$ . The ablation trace would certainly be the fingerprint of the generation of periodically enhanced near-field on the target surface during the interaction of surface with fs laser pulses. The above results suggest that the fine nanostructure should be formed through non-thermal process at low fluence, similarly for DLC and TiN [3,15]. A higher fluence would produce excess thermal energy in the surface layer to disturb the formation of the fine periodic structure, even if the periodically enhanced near-field is created in the interaction.

In the following we restrict our discussion to the fine structure formation process. The experimental results obtained may allow us to model the nanostructuring process of Si, using the physical process that we have recently proposed with respect to DLC [17,18].

When Si surface is irradiated with fs laser pulses, free electrons are produced in the surface layer. Since the present experiment employs a low fluence so that Si surface starts to be ablated with superimposed multiple shots of laser pulses, the target surface before ablation should undergo a bonding structure change. In fact, it is well known that crystalline Si irradiated with fs laser pulses is modified into amorphous Si (a-Si) [20]. In the present experimental conditions, we may expect that the a-Si layer would be formed on the target surface by the superimposed multiple shots of fs laser pulses before ablation.

For simplicity to illustrate the nanostructuring process, we assume that two layers consisting of the upper a-Si and lower Si layers are formed on the target surface just before ablation, as illustrated in the inset of Fig. 4. The ablation is initiated on the modified surface layer where a high density of free electrons is produced with the fs laser pulse. The generation of high-density free electrons should lead to a rapid and a large change in the dielectric constant of the upper a-Si layer during the ultrafast interaction with the target. In the most initial stage of ablation, a small

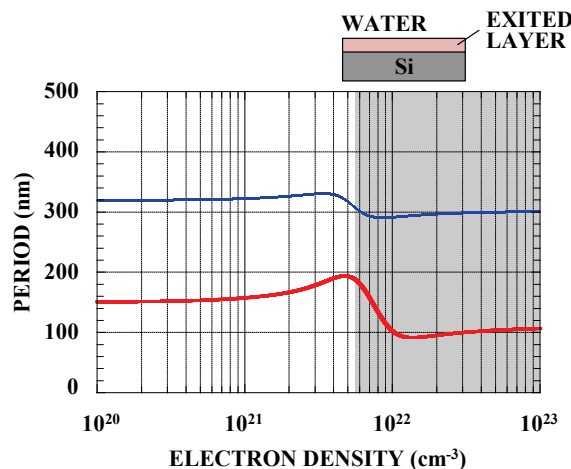


**Fig. 4** Near-field period calculated as a function of  $N_e$  for the interfaces of water/a-Si (upper blue curve) and a-Si/Si (lower red curve). The hatched part denotes the region of  $\epsilon' < 0$ .

number of  $N$  at a low fluence would first produce a weakly corrugated coarse structure on the surface, as seen in Fig. 1(a). The corrugated structure is able to couple the incident fs pulse with the SPPs. The SPPs can be excited at the interfaces between water and the a-Si layer and also between the a-Si layer and the Si substrate with subsequent pulses.

With the dispersion relation of the surface plasmons [21], the surface plasmon wave number  $k_{sp}$  is expressed as  $k_{sp} = k_0[\epsilon_{\text{water}} \epsilon' / (\epsilon_{\text{water}} + \epsilon')]^{1/2}$ , where  $k_0$  is the wave number of the incident light in vacuum,  $\epsilon_{\text{water}}$  and  $\epsilon'$  are the relative dielectric constants of water  $\epsilon_{\text{water}} = 1.76$  at 800 nm [22] and the a-Si layer including the effect of free electron, respectively. The SPPs produce periodically enhanced near-field at the interfaces to induce local ablation at a spatial period  $2\pi/(2\text{Re}[k_{sp}])$ .

Using the Drude model,  $\epsilon'$  in the laser field is given by  $\epsilon' = \epsilon - \omega_p^2 / (\omega^2 + i\omega\tau)$ , where  $\epsilon$  is the static relative dielectric constant of the target surface,  $\omega$  is the frequency of the incident light in vacuum,  $\tau$  is the Drude damping time, and  $\omega_p = [e^2 N_e / (\epsilon_0 m^* m)]^{1/2}$  is the plasma frequency with dielectric constant of vacuum  $\epsilon_0$ , electron charge  $e$ , electron density  $N_e$ , free electron mass  $m$ , and optical effective mass of carriers  $m^*$ . In the calculation for the incident laser wavelength of 800 nm, we used the following values:  $\epsilon = 13.5 + i0.0384$  for Si [23];  $\epsilon = 14.9 + i0.627$  for a-Si [24],  $m^* = 0.2$  for Si [25] and a-Si, and  $\tau = 1$  fs [26].

Figure 4 shows the period  $d$  calculated as a function of  $N_e$  for the interfaces of water/a-Si (upper blue curve) and a-Si/Si (lower red curve). The SPPs can be excited in the region of  $N_e > 5.5 \times 10^{21} \text{ cm}^{-3}$  that is hatched in Fig. 4, where  $\epsilon'$  is negative. The near-field period calculated for the a-Si/Si interface is in the range of  $d_{\text{cal}} = 100 - 200$  nm. Despite the simple model, the calculated result is in good agreement with the observed fine period of  $d \sim 150$  nm.

Although discussion on the interaction process for the coarse periodic structure formation at  $d \sim 400$  nm is beyond the scope of this paper, the experimental results suggest the ripple formation due to optical interference of the incident laser radiation with scattered and/or diffracted electromagnetic wave on the surface [27], or the interference process including the surface plasmons can produce sub-wavelength ripples as small as  $\sim \lambda/2$  [28,29].

Also we notice that thermal process play an important role in the formation of the coarse structure, as well as in the suppression of fine-structure formation.

#### 4. Conclusions

We have experimentally studied nanostructuring of Si surface irradiated in water with fs laser pulses. The results have shown that the fine nanostructure with  $d \sim 150$  nm can be produced in a restricted condition of small laser fluence, and the fine structure is developed from the initial coarse periodic structure with  $d \sim 400$  nm. The fine structure formation process has been modeled and analyzed with our model of the periodically enhanced near-field through the excitation of SPPs. The characteristic fine period of nanostructure observed is in good agreement with the calculation.

#### References

- [1] J. Reif, F. Costache, M. Henyk, S. V. Pandelov: Appl. Surf. Sci. 197-198, (2002), 891-895.
- [2] N. Yasumaru, K. Miyazaki, and J. Kiuchi: Appl. Phys. A 76, (2003), 983-985; 79, (2004), 425-427.
- [3] N. Yasumaru, K. Miyazaki, and J. Kiuchi: Appl. Phys. A 81, (2005), 933-937.
- [4] Y. Dong and P. Molian: Appl. Phys. Lett. 84, (2004), 10-12.
- [5] A. Borowiec and H. K. Haugen: Appl. Phys. Lett. 82, (2003), 4462-4464.
- [6] G. Daminelli, J. Krüger, and W. Kautek: Thin Solid Films, 467, (2004), 334-341.
- [7] R. Le Harzic, H. Schuck, D. Sauer, T. Anhut, I. Riemann, and K. König: Opt. Express, 13, (2005), 6651-6656.
- [8] M. Shen, J. E. Carey, C. H. Crouch, M. Kandyla, H. A. Stone, and E. Mazur: Nano Lett., 8, (2008), 2087-2091.
- [9] C. Wang, H. Huo, M. Johnson, M. Shen, and E. Mazur: Nanotechnology, 21, (2010), 075304.
- [10] R. Buividas, L. Rosa, R. Šliupas, T. Kudrius, G. Šlekys, V. Datsyuk, and S. Juodkakis: Nanotechnology, 22, (2011), 055304.
- [11] Q. Z. Zhao, S. Malzer, and L. J. Wang: Opt. Lett. 32, (2007), 1932-1934; A. Y. Vorobyev and C. Guo: J. Appl. Phys. 104, (2008), 063523.
- [12] E. V. Golosov, V. I. Emel'yanov, A. A. Ionin, Yu. R. Kolobov, S. I. Kudryashov, A. E. Ligachev, Yu. N. Novoselov, L. V. Seleznev, and D. V. Sinityn: JETP Lett. 90, (2009), 107-110.
- [13] Y. Shimotsuma, P. G. Kazansky, J. Qiu, and K. Hirao: Phys. Rev. Lett. 91, (2003), 247405.
- [14] V. R. Bhardwaj, E. Simova, P. P. Rajeev, C. Hnatovsky, R. S. Taylor, D. M. Rayner, and P. B. Corkum: Phys. Rev. Lett. 96, (2006), 057404.
- [15] K. Miyazaki, N. Maekawa, W. Kobayashi, N. Yasumaru, and J. Kiuchi, Appl. Phys. A, 80, (2005), 17-21.
- [16] G. Miyaji, K. Miyazaki: Appl. Phys. Lett., 89, (2006), 191902.
- [17] G. Miyaji, K. Miyazaki: Appl. Phys. Lett., 91, (2007), 123102.
- [18] G. Miyaji, K. Miyazaki: Opt. Express, (2008), 16265-16271.
- [19] G. Miyaji, K. Miyazaki: Appl. Phys. A, 98, (2010), 927-930.
- [20] J. Bonse, S. Baudach, J. Krüger, W. Kautek, and M. Lenzner: Appl. Phys. A, 74, (2002), 19-25.
- [21] H. Raether: "Surface Plasmons on Smooth and Rough Surfaces and on Gratings" (Springer, Berlin, 1988), p.5.
- [22] M. R. Querry, D. M. Wieliczka, and D. J. Segelstein: "Handbook of Optical Constants of Solids", edited by E. D. Palik and G. Ghosh (Academic, London, 1997), p.1059-1077.
- [23] J. Geist: "Handbook of Optical Constants of Solids", edited by E. D. Palik and G. Ghosh (Academic, London, 1997), p.519-529.
- [24] H. Piller: "Handbook of Optical Constants of Solids", edited by E. D. Palik and G. Ghosh (Academic, London, 1997), p.571-586.
- [25] H.M. van Driel: Appl. Phys. Lett., 44, (1984), 617-619.
- [26] K. Sokolowski-Tinten and D. von der Linde: Phys. Rev. B, 61, (2000), 2643-2650.
- [27] D. Bäuerle: "Laser Processing and Chemistry" (Springer, Berlin, 1996), Chap.28.
- [28] J. Bonse, A. Rosenfeld, and J. Krüger: J. Appl. Phys. 106, (2009), 104910.
- [29] M. Huang, F. Zhao, Y. Cheng, N. Xu, and Z. Xu: ACS Nano, 3, (2009), 4062-4070.

(Received: June 29, 2011, Accepted: April 16, 2012)